A Phase 2 Study of the Efficacy and Safety of Oral Selinexor in Recurrent Glioblastoma

Data Supplement

Contents

Supplemental Methods

Exploratory Molecular Correlative Studies

Antibodies used for immunostaining included Ki67 (Cell Marque, Cat No. 275R-18), FOXO1 (Cell Signaling Technology, Cat No. 2880), PTEN (Cell Signaling Technology, Cat No. 9188), cleaved caspase 3 (Cell Signaling Technology, Cat No. 9661), TP53 (Santa Cruz Biotechnology, Cat No. sc-126), and NGFR (Abcam, Cat No. ab3125). IHC stained slides were scanned with Aperio AT Turbo scanner at 20X to generate digital images. Percentage of positive cells in Ki67 and cleaved caspase 3 stained samples were determined using Aperio image analysis software. Average and standard deviation were calculated from three representative areas analyzed for each stain.

Ribodepleted RNA sequencing (RNAseq) and exome sequencing were performed on archival tumors from 57 patients and post-selinexor treatment resected tumors from 3 patients (Arm A) by HudsonAlpha Discovery Sequencing and Bioinformatics Division (Huntsville, AL). Exome sequencing reads were aligned using Burrows-Wheeler Alignment,(1) and variants were called using Genome Analysis Toolkit's Mutect2.(2) Variants with allele frequencies <0.1, read depth <8 reads, within the immunoglobin gene regions, and common polymorphisms with global minor allele frequencies > 0.01 were filtered. RNAseq reads were aligned with HiSAT2,(3) then gene-level expressions were determined with featurecounts.(4) Gene expression normalization and comparison was performed with DeSeq2.(5) RNAseq data were used to infer the activities of 6,203 regulatory proteins, including proteins annotated as Transcription Factors (GO:0003700, or GO:0004677 and GO:0030528 or GO:0045449), co-Transcription Factors (GO:0003712 or GO:0030528 or GO:0045449), and signaling proteins (GO:0007165 and GO:0005622 or GO:0005886) in Gene Ontology.(6) Protein activity was measured by Virtual Inference of Protein-activity by Enriched Regulon analysis (VIPER), which converts tumor sample gene-

expression profiles into accurate protein activity profiles,(7) using a GBM context-specific model of transcriptional regulation (interactome) available from Bioconductor (https://www.bioconductor.org/packages/release/data/experiment/html/aracne.networks.html). VIPER-inferred protein activity is approved by the New York State Department of Health CLIA/CLEP Validation Unit as an offering in the category of "Molecular and Cellular Tumor Markers for Oncology.(8)

Five machine learning algorithms, including linear discriminant analysis (LDA), logistic regression, ridge regression, neural networks, and random forests, were used to train classifiers, based on the top k = 1, …, 10 most differentially active proteins between samples from patients who most clearly benefitted from treatment (best overall response [BOR] of complete response or partial response, or durable stable disease with progression-free survival [PFS] >140 days) and patients resistant to treatment (BOR of progressive disease or PFS <100 days). Five samples, corresponding to resistant patients, were not used for molecular correlative studies as they were identified as outliers by unsupervised analysis based on the top three principal components' projection of the data (capturing 69% of the data variance), and by supervised analysis including all 6,203 evaluated proteins. Leave-one-out cross-validation (LOOCV) was used to estimate the optimal number of features (k = 3) and a biomarker model was assembled by integrating the quantile-transformed-scores (copula transformation) generated by each of the individual machine learning algorithms. This ensemble model approach has been previously described and shown to generally outperform the predictions from individual models.(9) The same ensemble approach, based on the quantiles from the training set, was used to integrate the predictions for an internal validation set, composed of 11 samples from patients considered selinexor resistant (BOR of PD or non-durable SD) or sensitive (BOR of durable SD).

Selinexor Pharmacokinetic assessment

In Arm A of the study, blood samples were collected pre-dose on the day of surgery and at 1-hour and 2-hour (at approximately the same time as resection of the tumor tissue) post-dose. Blood samples were collected in K_2EDTA plasma separator tubes, centrifuged for plasma within 30 minutes of collection, and stored at - 80°C. Tumor tissue samples obtained upon cytoreductive surgery were flash frozen in liquid nitrogen and stored at or below -70°C. Plasma and tumor samples were analyzed for concentrations of selinexor by protein precipitation extraction followed by analysis with liquid chromatography and tandem mass spectrometry (LC/MS/MS). The quantification range for selinexor is 1.00 to 1000 ng/mL.

Up to 3 doses of selinexor were administered starting up to 12 days pre-operatively (originally at 50mg/m2 twice weekly which was also the schedule for the Arm B non-surgical cohort) to allow flexibility with regard to scheduling of surgery that could occur with varying levels of urgency in clinical practice. In this way, all patients received at least 1 pre-operative dose but were allowed up to 3 if the date of surgery were more than a few days from enrollment (**Table S2**). The final pre-surgical dose was intended to be taken 0-4 hours prior to surgery, as selinexor reaches peak serum concentrations in 2-4 hours and the half-life is 6-7 hours.(10)

Supportive care

Selinexor was to be taken orally within approximately 30 minutes of a light meal with approximately 4 oz of water. Moderate to severe fatigue and gastrointestinal side effects (i.e., anorexia, nausea/vomiting, diarrhea) which were expected side effects, were managed with dose reductions or delays as needed. Anti-emetic prophylaxis was required for all doses, with other supportive measures to manage GI toxicities as needed (such as appetite stimulants

including megesterol, glucoroticoids, and others). Hematologic toxicities, particularly thrombocytopenia as an agent-related adverse event, was managed with dose reduction, delays, and transfusion if needed.

Table S1: Efficacy outcomes in mITT population

	Arm B (N = 24)	Arm C (N = 13)	Arm D (N = 30)
6-cycle PFS* %, (95% CI)	14.6 (5.3 - 40.2)	7.7 (1.2 - 50.6)	27.6 (15.3 - 49.8)
Progression Free at 6 Cycles, n (%)	3 (12.5)	1 (7.1)	8 (26.7)

CI, confidence interval; PFS, progression-free survival; *survival rate point estimates are using the Kaplan-Meier method. Excludes one patient from Arm C who did not undergo efficacy evaluation.

Table S2: Median Time on Selinexor and Progression-free Survival by Study Arm

	Arm B (n = 24)	Arm C (n = 14)	Arm D (n = 30)
Median PFS, months	1.6	1.9	1.9
Median time on selinexor, months (IQR)	1.4 (0.3)	1.8 (0.1)	1.8 (0.6)

IQR, interquartile range; PFS, progression-free survival

Table S3. Concomitant Dexamethasone Administration

Arm	Patient	Largest reduction in tumor from baseline (%)	Study day of largest reduction	Reason for dexamethasone treatment	Dexamethasone dose per administration (mg)	Study day dexamethasone started
B	1	-30.7	84	Peri-tumoral edema	1.5	-46
				Nausea prophylaxis	4	1
				Peri-tumoral edema	1	11
				Peri-tumoral edema	0.5	19
				Edema prophylaxis	2	43
				Edema prophylaxis	1.5	48
	2	-39.5	147	Nausea prevention	4	1
	3	-15.8	56	Prophylaxis symptoms of cerebral edema	4	-70
	4	-32.4	44	-	-	-
	5	-100.0	49	-	-	-
	6	-78.0	51	-	-	-
C	7	-12.7	21	Cerebral edema (secondary GBM)	8	-44
	8	-100.00	103	Nausea	4	141
	9	-20.8	111	GBM	2.5	-49
				Prophylactic selinexor dosing	4	1
				GBM	3	96
				GBM	2	113
				Prophylactic selinexor intake	3	113
	10	-23.5	112	GBM	3	-10
				GBM	6	77
	11	-71.4	111	GBM	2	1
	12	-1.2	56	Headache	4	-106
				Prophylaxis	4	8
				Headache	2	51
D	13	-76.3	728	Cataract surgery-left eye	1	596
				Cataract surgery-right eye	1	609
	14	-100.0	112	Nausea	4	57
				Nausea	4	141
	15	-18.0	63	Cerebral edema	2	-26
				Cerebral edema	3	86
				Cerebral edema	2	99
	16	-7.1	54	Prophylaxis	4	-1
	17	-95.9	384	Vomiting	3.5	-9
	18	-10.5	112	-	-	-
	19	-55.4	49	-	-	-

Table S4. Selinexor concentrations in resected tumor samples within 6 hours of last pre-operative selinexor dose

Patient (Arm A)	Selinexor pre-op dosing at 50mg/m2 body surface area [days]								Time between surgery and last pre-surgical dose (hours:minutes)	Tissue Weight (g)	Tumor selinexor concentration		Tumor/Plasma ratio	Plasma selinexor concentration					
														predose		1h		2h	
	-12	-10	-7	-6	-5	-4	-1	0			ng/g	nM		ng/mL	nM	ng/mL	nM	ng/mL	nM
1				X		X		X	2:37	0.3582	93.6	211	-	BLQ		263	593	-	-
2								X	2:56	0.664	62.8	142	0.0875	BLQ		918	2071	718	1620
3			X					X	2:48	0.938	30.5	68.8	0.0953	BLQ		458	1033	320	722
4								X	3:37	0.570	28.3	64	0.0765	BLQ		437	986	370	835
5								X	3:55	0.671	17.6	39.7	0.0616	BLQ		138	311	286	645
6				X		X		X	4:38	0.612	129	291	0.190	1.34	3.02	-	-	678	1529

BLQ, below limit of quantification; -, data not available.

Figure S1. Complete response

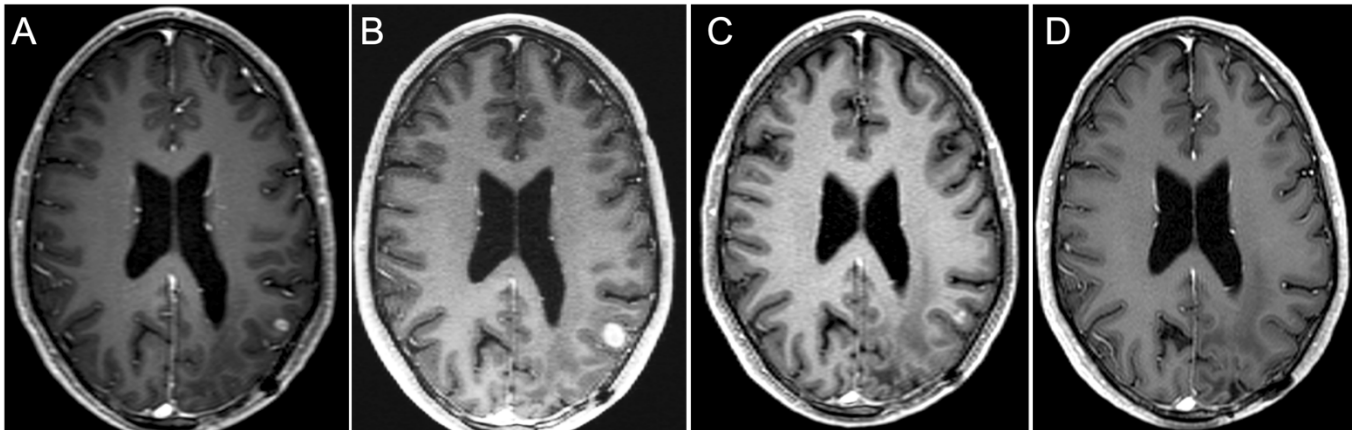

Figure S1. Magnetic resonance contrast-enhanced axial T1 images taken throughout the course of treatment are shown 7 weeks before selinexor *(A)*, at baseline 1 week before selinexor (*B*), and during a partial response after 16 weeks of treatment (*C*), and then complete (*D*) response beginning after 24 weeks of treatment and confirmed after of 32 weeks of treatment (not shown). The patient was a 36-year-old man with *IDH* wild-type *MGMT* promoter methylated GBM, treated with selinexor on Arm D, given as second-line therapy after progression of disease to radiotherapy and temozolomide.

Figure S2. Durable partial response

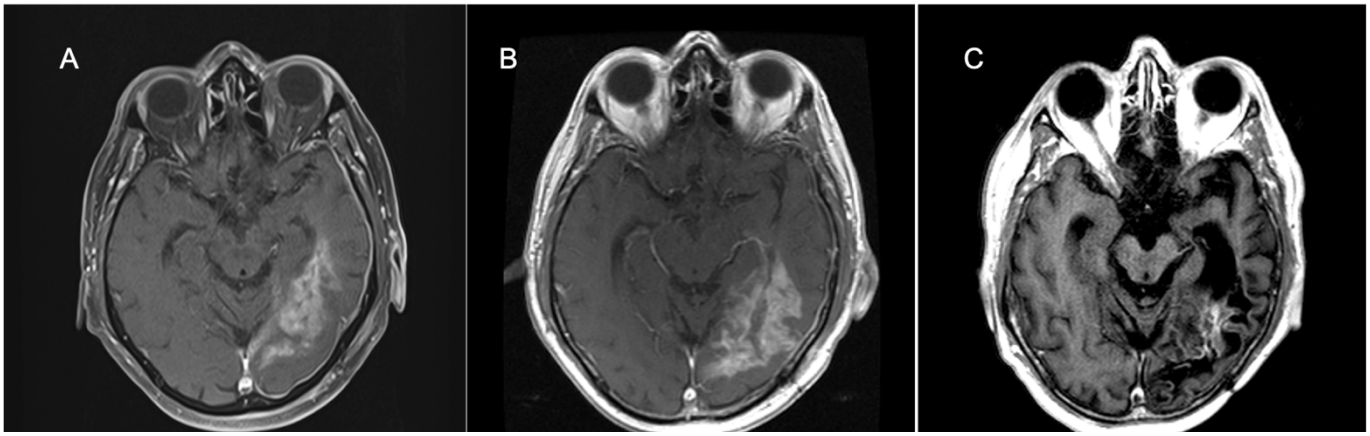

Figure S2. Magnetic resonance contrast-enhanced axial T1 images taken throughout the course of treatment are shown after subtotal resection of recurrent GBM (*A*), and further increase in tumor size ~3 weeks after the post-operative MRI as a new baseline (*B*), the patient received selinexor on Arm D, and a durable partial response (*C*) was observed beginning ~73 weeks after starting selinexor with a maximum tumor size reduction of 72%. At the time of data lock, treatment of this patient continued through Karyopharm's Expanded Access Program (KEAP), and he remained in a partial response after 42 months of selinexor when data collection ceased. The patient was a 64-year-old man with *IDH* wild-type and *MGMT* promoter unmethylated GBM, treated with selinexor on Arm D, given as third-line after progression of disease despite radiotherapy and temozolomide (first-line) and experimental AKT inhibitor combined with mTOR inhibitor (second-line).

Figure S3.

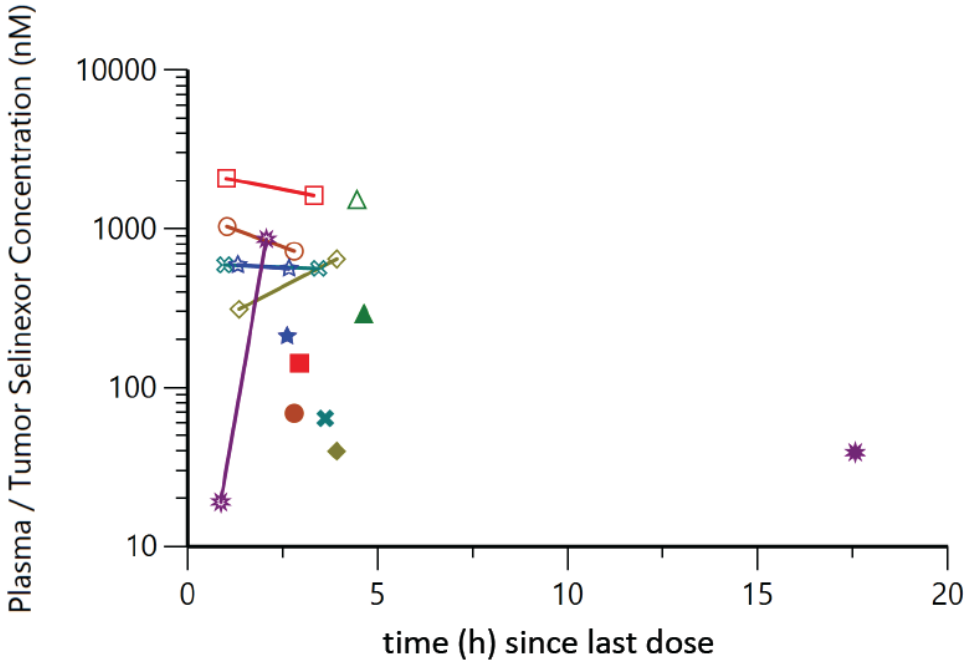

Figure S3. Plasma and intra-tumoral concentrations of selinexor after last dose. Lines show the plasma selinexor concentration in 7 patients enrolled on Arm A, with each patient represented by a different shape and color. Individual points represent the intra-tumoral concentration of selinexor from resected tumors. Lines and points are plotted according to time since last dose of selinexor. Open symbols represent plasma concentrations and closed symbols tumor concentrations.

Figure S4

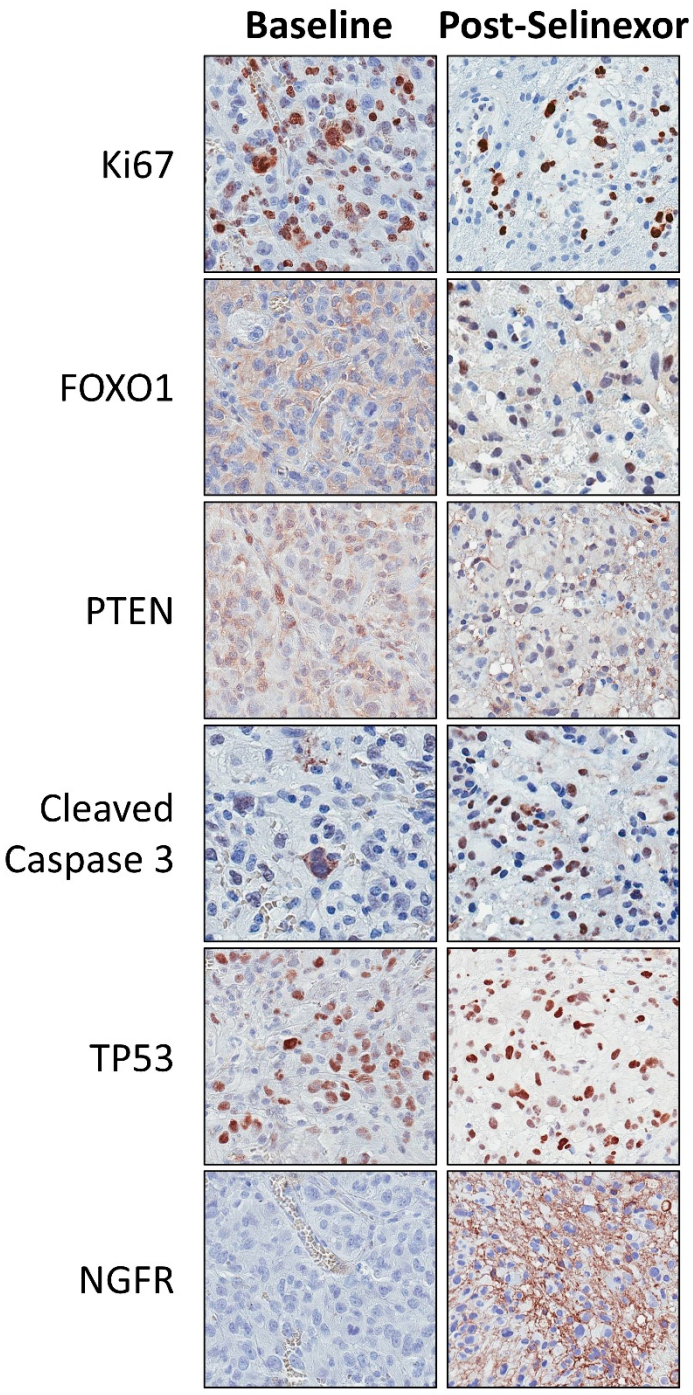

Figure S4. Immunohistochemistry from pre- and post- selinexor treatment. Baseline sample from patient A-3 collected on day -70, and post-treatment sample collected during surgery that began 2h 56min after first selinexor dose was orally administered. Decreased cell proliferation (Ki67), increased apoptosis (cleaved caspase 3), and increased nuclear retention of major tumor suppressor proteins FOXO1, p53, PTEN are evident after selinexor treatment. NGFR also significantly increased post-selinexor treatment.

Figure S5

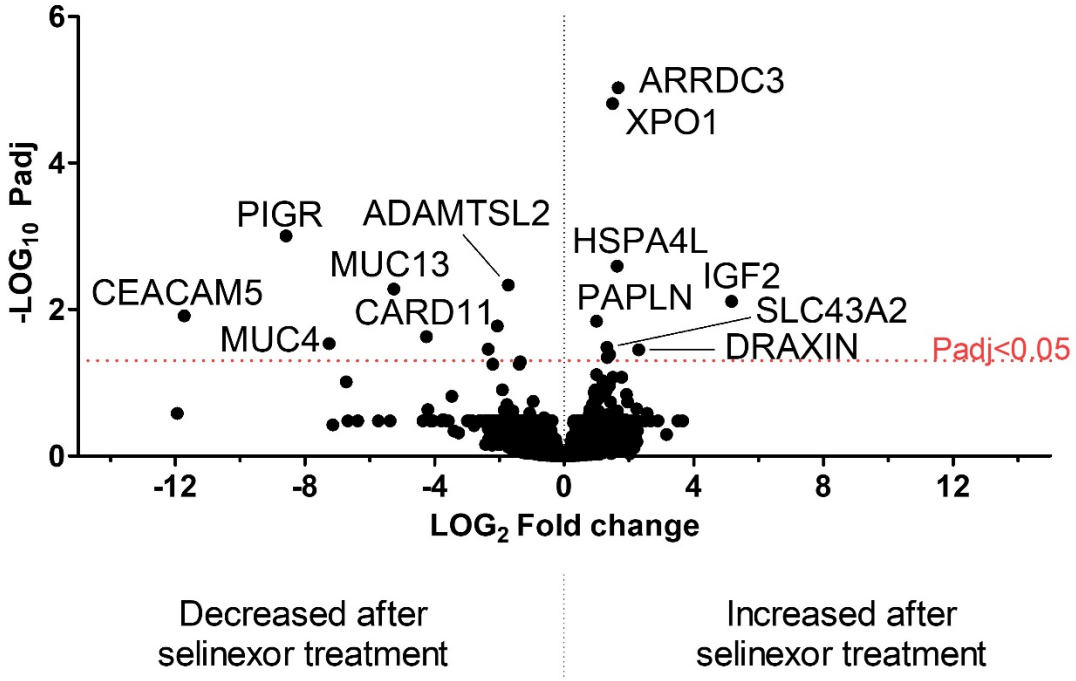

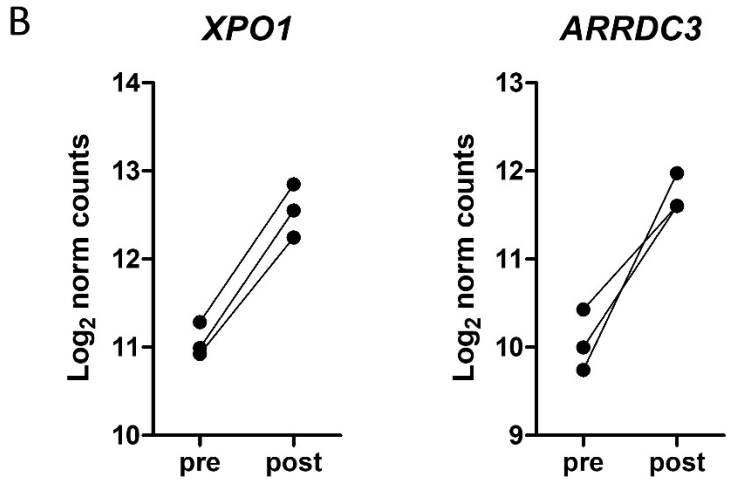

Figure S5. Differentially expressed genes between pre- and post- selinexor treated tumors. A. Volcano plot shows expression differences from resected post-selinexor treatment tumors from three patients treated on Arm A compared to archival tumor specimens from these patients. Significance (adjusted for multiple comparisons) is shown on the y-axis, and fold-change on the x-axis for all detectable genes (base mean > 100). **B**. Dot plots show paired pre- and post- treatment tumor expressions of *XPO1* and *ARRDC3*, which were the most significantly differentially expressed genes.

Figure S6.

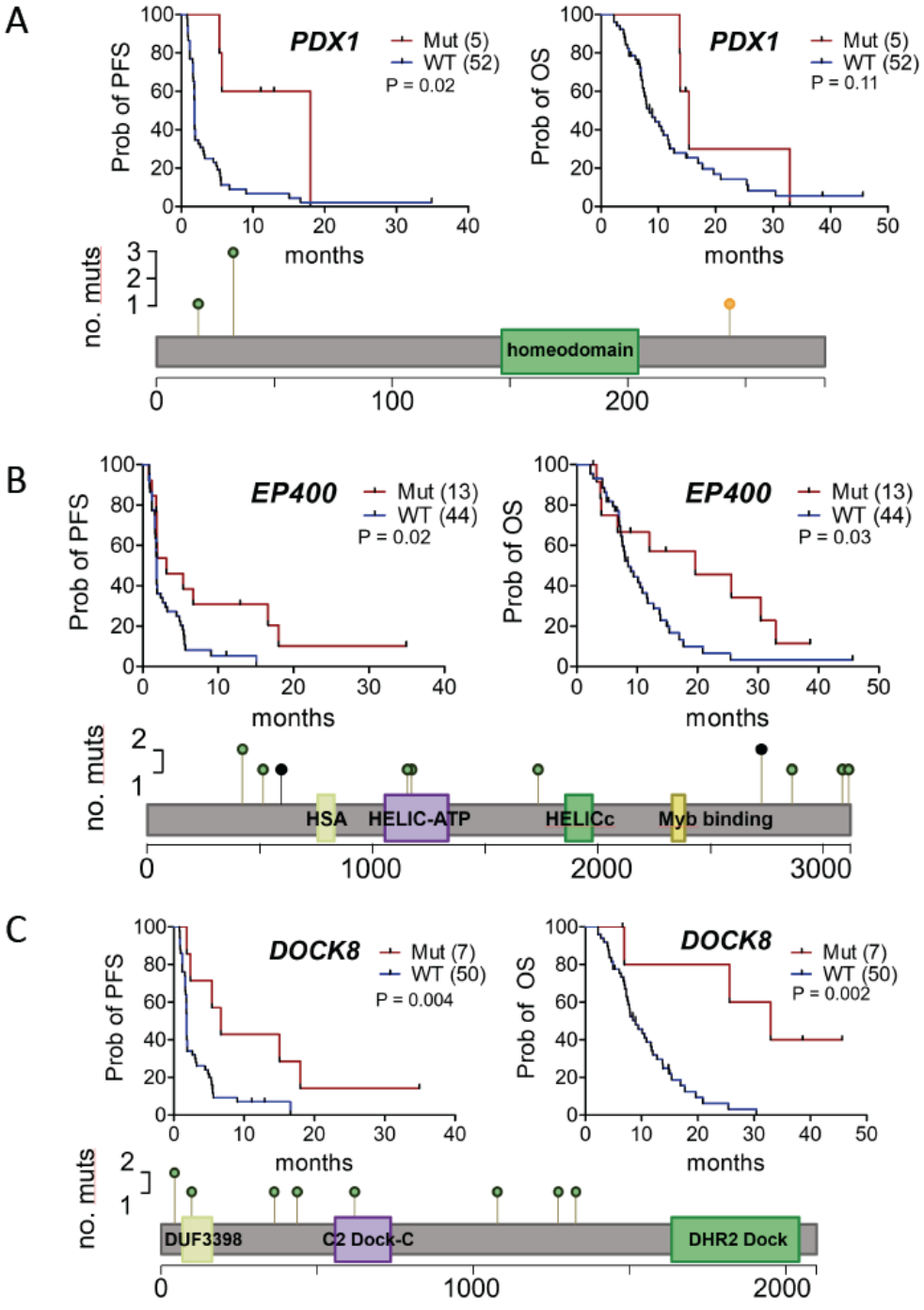

Figure S6. Mutations associated with benefit from selinexor. Progression-free survival (PFS) and overall survival (OS) curves shown for mutant (Mut) and wild-type (WT) patients for the indicated genes. P-values calculated with log-rank tests. Below each set of curves, lollipop plots show the identified mutations and protein domains (green, missense; orange, in-frame indel; black, nonsense or frameshift). Mutations visualized with the Lolliplot R package.

Figure S7.

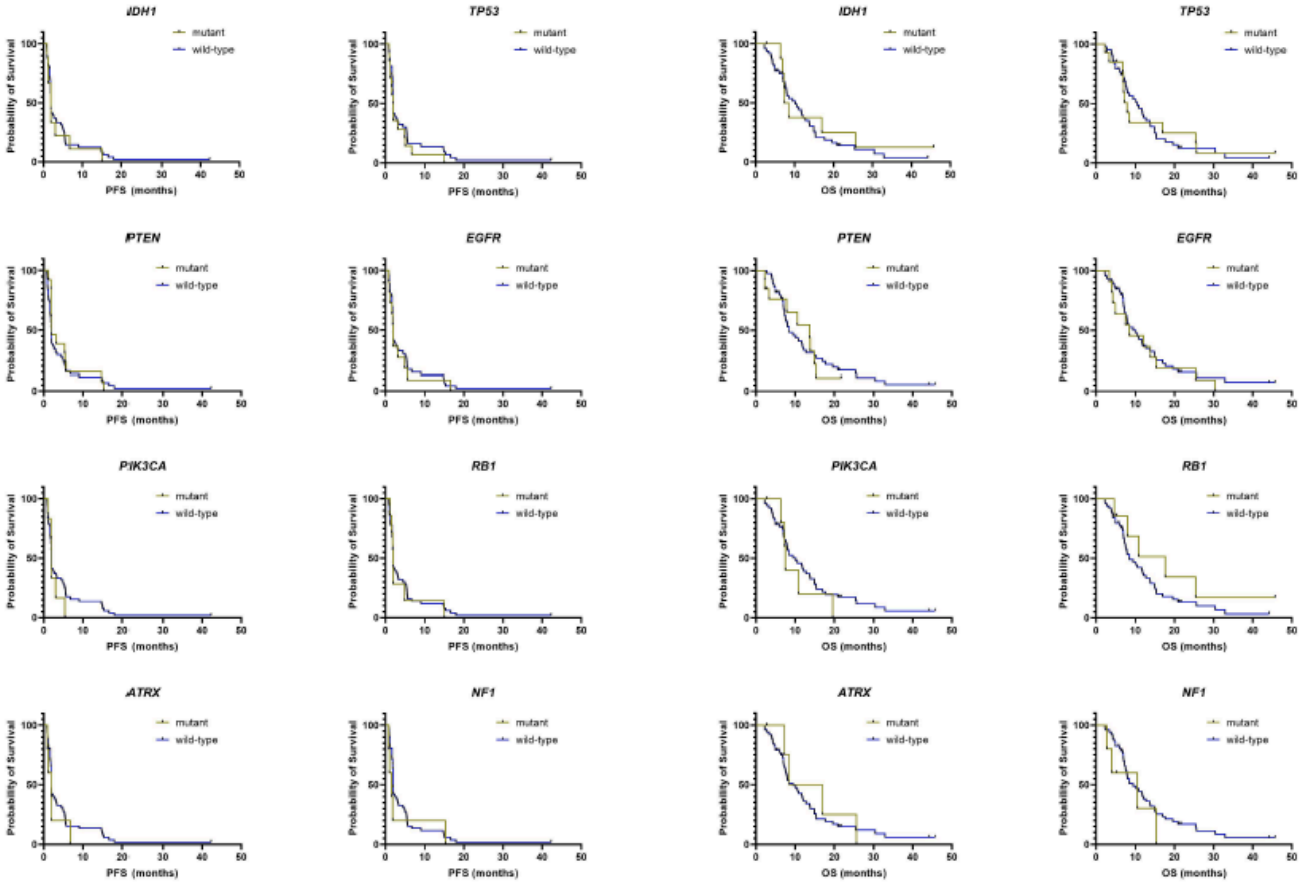

Figure S7. Survival stratified by common molecular abnormalities. Progression-free survival (PFS) and overall survival (OS) curves stratified by mutations, chromosomal losses and protein expressions typically evaluated in patients with glioblastoma.

Figure S8.

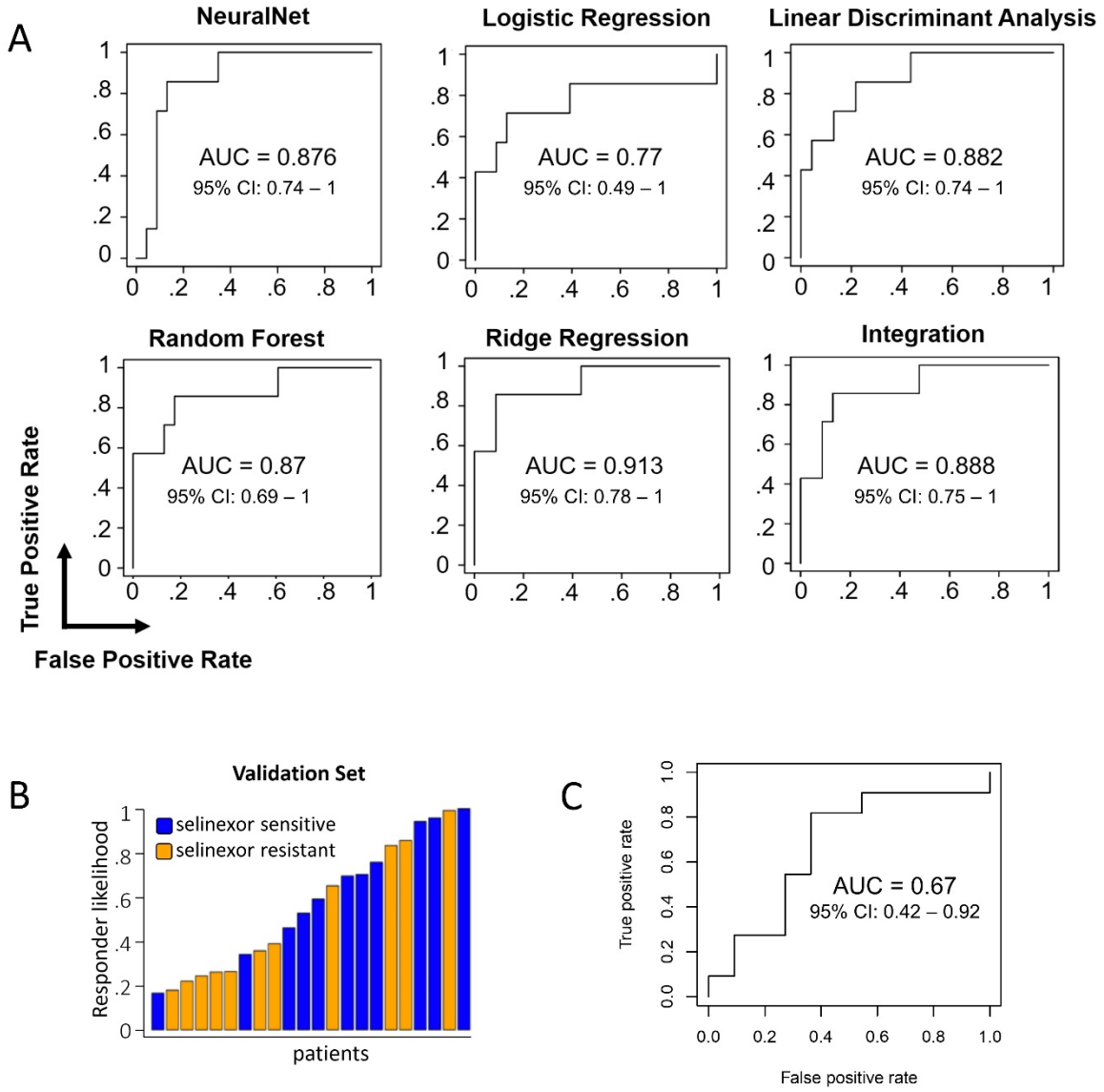

Figure S8. Machine learning models using inferred protein activity to predict selinexor sensitivity. A. Receiver operating characteristic (ROC) curves for the "Discovery" set of responders (patients with best overall RANO-response of partial or complete response) and resistors (best overall response progressive disease despite at least 30 days of treatment) illustrate the predictive power of an activity score of three proteins (RAB43, SOCS3, and ZC3H12A) for the indicated machine learning models and an ensemble model generated by their integration. **B.** Bar plot showing the predicted probabilities of benefit (selinexor sensitive, best RANO-response of stable disease durable for at least 140 days) vs. lack of benefit (selinexor resistant, best RANO-response of stable disease durable for less than 100 days or progressive disease but after less than 30 days of drug exposure) using the integrated model based on the inferred activity for three-proteins in the internal "Validation" set of cases. **C.** ROC analysis for the internal "Validation" set. Area Under the Curve (AUC) and 95% Confidence Intervals (CI) are indicated in the figure.

References

1. Li H, Durbin R. Fast and accurate short read alignment with Burrows-Wheeler transform. Bioinformatics. Bioinformatics; 2009;25:1754–60.
2. McKenna A, Hanna M, Banks E, Sivachenko A, Cibulskis K, Kernytsky A, et al. The genome analysis toolkit: A MapReduce framework for analyzing next-generation DNA sequencing data. Genome Res. Genome Res; 2010;20:1297–303.
3. Kim D, Langmead B, Salzberg SL. HISAT: A fast spliced aligner with low memory requirements. Nat Methods. Nature Publishing Group; 2015;12:357–60.
4. Liao Y, Smyth GK, Shi W. FeatureCounts: An efficient general purpose program for assigning sequence reads to genomic features. Bioinformatics. Oxford University Press; 2014;30:923–30.
5. Love MI, Huber W, Anders S. Moderated estimation of fold change and dispersion for RNA-seq data with DESeq2. Genome Biol. BioMed Central Ltd.; 2014;15.
6. Ashburner M, Ball CA, Blake JA, Botstein D, Butler H, Cherry JM, et al. Gene Ontology: tool for the unification of biology. Nat Genet 2000 251. Nature Publishing Group; 2000;25:25–9.
7. Alvarez MJ, Shen Y, Giorgi FM, Lachmann A, Ding BB, Hilda Ye B, et al. Functional characterization of somatic mutations in cancer using network-based inference of protein activity. Nat Genet. Nature Publishing Group; 2016;48:838–47.
8. Neal M. Assay Validation Review. New York; 2019. Report No.: Project ID: 63859.
9. Ahsen ME, Vogel RM, Stolovitzky GA. Unsupervised Evaluation and Weighted Aggregation of Ranked Classification Predictions. J Mach Learn Res. 2019;20:1–40.
10. Abdul Razak AR, Mau-Soerensen M, Gabrail NY, Gerecitano JF, Shields AF, Unger TJ, et al. First-in-Class, First-in-Human Phase I Study of Selinexor, a Selective Inhibitor of Nuclear Export, in Patients With Advanced Solid Tumors. J Clin Oncol. 2016;34:4142–50.